Mechanism of photochemical degradation of Fe(III)-EDDS complex

S. Jaber, M. Leremboure, V. Théry, A.-M. Delort, G. Mailhot

Mechanism of photochemical degradation of Fe(III)-EDDS complex

S. Jaber [1], M. Leremboure [1,2], V. Thery[1], A.-M. Delort [1], G. Mailhot [1*].

(1) Université Clermont Auvergne, CNRS, SIGMA Clermont, Institut de Chimie de Clermont-Ferrand (ICCF), 63000 Clermont-Ferrand, France.

(2) Université Clermont Auvergne, UCA-PARTNER, Mass Spectrometry Facility, 63000 Clermont-Ferrand, France.

* Corresponding author:

E-mail address: gilles.mailhot@uca.fr

Keywords: Iron complexes, Photochemistry, Mass spectrometry, Radical chemistry, EDDS

Abstract

In this work, we investigated the photochemical degradation of the complex Fe(III)-EDDS which is increasingly used in studies of advanced oxidation processes. After irradiation of the aqueous solution, HPLC-HRMS analyses are used to identify the degradation products of EDDS. Six different products are separated and identified with specific chemical formulas. Proposed mechanisms based on the initial photo-redox process can explain the formation of all the products. They correspond to oxidized products with a shorter carbon chain and aldehyde and/or carboxylic acid functions. Among, them the formation of formaldehyde is also proposed in the mechanisms. This study is the first one that identifies degradation products of Fe(III)-EDDS complex and proposes a complete mechanism of degradation that can be applied for other iron complexes.

Keywords:

Iron complex; EDDS; Photochemistry; Oxidation; Radical chemistry; Mass spectrometry

1. Introduction

Chelating agents, chemical compounds in which two or more electron donor groups form a complex with polyvalent metal, are increasingly used for a long time in different applications. The first application was in medicine and developed after the Second World War for treating arsenic contamination by war gas poisoning [1]. This first application was shortly followed by the use of ethylenediaminetetraacetic acid (EDTA) which was used to remove heavy metals (aluminum, lead, mercury, copper, etc.) from the human body [2]. So the interest for the chelation therapy in the removal of metal was strongly developed to treat different pathologies between the 60's and the 80's. After this period, chelating agents were mainly used for non-invasive diagnostic medicine in different applications such as the vectorization of cations to specific part of the body and in the manipulation of nucleic acids. Environmental contamination by metals and use in detergents or pulp and paper industry were the second domain of applications of organic chelating agents more particularly with EDTA [3]. In the soil treatment the addition of chelating agent improves the metal accumulation in the plants and aminopolycarboxylic acids (APCAs) have been used in various phytoextraction experiments [4]. For water treatments, and more precisely in the advanced oxidation processes (AOPs), chelating agents were used due to the low or non-efficiency of the Fenton or photo-Fenton process at pH higher than 4.5. The presence of chelating agent avoids the precipitation of iron and the Fenton process can be observed at pHs until 9.0 [5]. Moreover, it is observed that the efficiency in terms of organic pollutant degradation was higher at higher pHs when Fe-Chelating agent complexes were involved [5, 6]. However, EDTA, the most used synthetic chelating agent, shows a high toxicity and very poor biodegradability while the biodegradable ethylenediamine-N,N'-disuccinic acid (EDDS) has been proposed as an alternative to EDTA and other persistent APCAs [4, 7]. In fact, different studies demonstrated that EDDS is highly biodegradable whatever its speciation, complexed with metal or free [8-

11] and so EDDS is considered as a safe and friendly chemical product for the environment. As a consequence, EDDS was used increasingly in consumer products (washing powders) or in soil washing effluent to favor the extraction of metals.

So due to the environmental and physicochemical properties of Fe(III)-EDDS complex, different research groups all over the world started to introduce this complex in AOPs especially in Fenton and photo-Fenton processes. The first studies started in the beginning of this century with 1 to 5 papers per year until 2010. Since that date we observe a strong increase of the number of papers with the words "EDDS" and "Fenton" in the topic of the paper (Figure 1). This trend is confirmed by two recent review articles of Clarizia et al. [12] and of Zhang and Zhou [13] on the Fenton or photo-Fenton processes at near neutral pH. In all these papers, the effect of the complex Fe(III)-EDDS on the Fenton and photo-Fenton processes was investigated in order to produce more radical species (hydroxyl radicals) with the goal to increase the degradation of organic pollutants in aquatic compartments [5, 6, 14]. The efficiency of the complex Fe(III)-EDDS was also tested for the treatment of municipal wastewater, for the disinfection of water but also for the photo-generation of sulfate radicals [15-17]. The effects of different parameters were studied and more particularly the pH and the natural inorganic ions (carbonate, chloride ions, …). The generation of different radical species ($^{\bullet}OH$, $SO_4^{\bullet-}$, $HO_2^{\bullet}/O_2^{\bullet-}$) was also well identified and characterized. Moreover, the chemical structure of Fe(III)-EDDS complex, the predominance of the different species and their photochemical efficiency were very well described [18]. However, to our knowledge, any study presents the fate of EDDS after the primary photoredox process involved in such iron complexes. One of the main study, and perhaps the only one, describing the first step of the photochemical process and the fate of the chelating agent is a work on the photochemical impact of the Fe(III)-nitrilotriacetic acid (NTA) complex on the 4-chlorophenol. Abida et al. [19] describe detailed mechanisms as a function of the irradiation wavelength including the

fate of the chelating agent. They identified the main transformation products of NTA, i.e. iminodiacetic acid and formaldehyde.

The objective of this work was to identify the primary transformation products of EDDS obtained after the photoredox process and describe the unknown photo-degradation pathways of this compound. The fate of the chelating agent is a crucial point of which the scientific community must be concerned if we want to generalize this type of iron complexes in the AOPs used for wastewater treatment.

2. Materials and Methods

2.1 Chemical

Ferric perchlorate hexahydrate 97% and S,S'-ethylenediamine-N,N'-disuccinic acid trisodium salt (EDDS-Na) solution (35% in water) were obtained from Sigma Aldrich, sodium hydroxide (NaOH) and perchloric acid ($HClO_4$) were obtained from Merck and used to adjust the pH of the solutions.

2.2 Complex Fe(III)-EDDS preparation

Fe(III)-EDDS complex 0.5 mM was prepared in Volvic® water, using an equimolar solution of Ferric perchlorate hexahydrate (100 mM) and S,S'-ethylenediamine-N,N'-disuccinic acid trisodium salt (100 mM). This preparation was performed in dark conditions to avoid potential photochemical reactions. The pH was adjusted to 6, using NaOH and $HClO_4$ solutions, and the complex solution was stored also in dark conditions for the same reason.

Before all the experiments, the concentration of the iron complex was controlled and evaluated by UV-visible spectroscopy by measuring the wavelength at 239 nm, one maximum of the Fe(III)-EDDS spectrum, corresponding to a molecular absorption coefficient ε equal to 8,400 M^{-1} cm^{-1} [20].

All the complex solutions were prepared in Erlenmeyer flasks, and the experiments were performed in an Infors® system at 17 ° C with shaking at 130 rpm. This system also allows irradiation.

2.3 Irradiation set up

The irradiations were performed in the Infors® system equipped with lamps Sylvania Reptistar (15W). The actinic flux was measured with an optical fiber and a charge-coupled device (CDC) spectrophotometer (Ocean Optics USD 2000 + UV-Vis). Lamps actinic flux was compared with emission solar spectrum (Fig. 2). The main advantage of using this kind of lamps was the good superimposition of the spectra in the shorter wavelength but also a lower intensity than the solar emission. Indeed, this lower intensity allows decreasing the rate of degradation of the Fe(III)-EDDS complex, in order to be able to detect more easily the primary products.

2.4 UPLC-HRMS Analysis

HPLC-HRMS (High Performance Liquid Chromatography-High Resolution Mass Spectrometry) analysis of Fe(III)-EDDS aqueous solution were performed using an UPLC RSLC (Ultra Performance Liquid Chromatography-Rapid Separation Liquid Chromatography) UltiMate™ 3000 (Thermo Scientific™) equipped with an Q Exactive™ Hybrid Quadrupole-Orbitrap™ High Resolution Mass Spectrometer (Thermo Scientific™) ionization chamber.

Chromatographic conditions

Chromatographic separation of the analytes was performed on a Kinetex® EVO C18 (1.7 µm, 100 mm × 2.1 mm, Phenomenex) column with column temperature of 30°C. The mobile phase was a mixture of water and acetonitrile, in gradient mode, at a flow-rate of 0.45 mL min^{-1}, with an injected volume of 5µL. The gradient elution program conditions are given in

Table S1. This device was coupled with a Thermo Scientific™ Dionex™UltiMate™ DAD 3000 UV-visible detector, using a wavelength range between 200-400 nm.

ESI Q-ORBITRAP™ parameters

The Q-Exactive ion source is equipped with electrospray ionization (ESI) and operates in full MS. The full MS scanning range is set between m/z 80 and 1200.The mass resolution was set to 70000 fwhm, the target AGC (automatic gain control) or the number of ions to be filled C-Trap has been set to 10^6 with a maximum injection time (IT) of 50 ms. The other generic Q-Exactive parameters were: N_2 gas flow rate set at 10 a.u, N_2 sheath gas flow rate set at 50 a.u, sweep gas flow rate set at 60 a.u. The spray voltage is of the order of 3.2 kV in positive mode and 3 kV in negative mode. The capillary temperature is at 320°C and the temperature of the heating element is at 400°C. Both positive and negative ionization modes are used.

Data Analysis and Visualization

Analysis and visualization of the data set were performed using Xcalibur™ 2.2 software; this software controls and processes data from Thermo Scientific ™ LC-MS systems and associated instruments.

2.5 Molecular modeling study

All computations were performed with GAUSSIAN 16 rev B01 [21]. The Functional Theory (DFT) [22, 23] level with unrestricted B3LYP [24–26] hybrid functional and 6-31G basis sets were used. The Implicit solvent method PCM [27] in water was applied. The thermodynamic corrections have been taken into account. All energy values presented in the results and discussion part are Gibbs free energy. For both minima, no imaginary frequencies were found. The chemical structure retained is the neutral form of the system with a formal charge of 0 and the multiplicity of spin equal to 2.

3. Results and discussion

3.1 Photodegratation of the iron complex

The kinetics of Fe(III)-EDDS photodegradation and of the byproducts formation are presented on the Figure 3. The detection of the compounds was performed using an UPLC-HRMS device.

Without irradiation, in the dark condition no significant degradation of the complex Fe(III)-EDDS is observed after 24 hours. On the contrary, under irradiation the Fe(III)-EDDS complex is decomposed with 60% and 80% of degradation after 3 and 5 hours of irradiation respectively. The degradation of the complex Fe(III)-EDDS is almost complete after 24 hours of irradiation.

During the irradiation, the formation of different photoproducts is observed by UPLC-HRMS, it is concomitant to the degradation of Fe(III)-EDDS. The UPLC chromatogram shows the appearance of several peaks among them two majors (c and d) and four smaller peaks (f, g, k and a) that we can measure easily (figures S1-S7). All of them have a very short retention time, lower than 1 min and close to that of Fe(III)-EDDS (0.64 min) (Table 1). According to the UPLC-HRMS analysis, four of the photo-products respond to the same ionization mode than EDDS (positive mode), two of them respond to the negative mode and all of them have a mass lower than that of the Fe(III)-EDDS complex (≈ 346 g mol^{-1}) and EDDS (≈ 292 g mol^{-1}) (Table 1 and Figure S1-S7).

All these observations confirm that the six main photo-products are fragments of EDDS, the organic ligand of the iron complex. All the information obtained by UPLC-HRMS on Fe(III)-EDDS complex, EDDS and the six photo-products are depicted in the table 1. The molecular formulas of the six photo-products have been identified, they still contain the two nitrogen atoms of EDDS. This result show that the primary (photo)-reactivity in the complex Fe(III)-EDDS does not involve the ethylene-diamine group. This observation is completely consistent

with mechanism described previously for Fe(III)-NTA complex [19]. The authors of this paper show that the first stage of the photochemical mechanism is the photoredox process between Fe(III) and one carboxylate group of NTA followed by a fast decarboxylation of the primary radical. In our case, the primary mechanism is thus located on the carboxylate groups and does not interfere on the center part of EDDS structure.

According to the results of LC-MS, two photoproducts are mainly formed: (c) and (d) (Figure 3). After 4 hours of irradiation of the Fe(III)-EDDS complex, the relative percentages of the formation of these fragments are within the range of 10% and 4% of the initial amount of the Fe(III)-EDDS complex. Other photoproducts are formed, but compared with photoproducts (c) and (d); the MS signals have a lower intensity. This can be explained by the potential mechanism detailed in the following part of the paper, showing all the pathways of Fe(III)-EDDS photodegradation mechanism and is supported by the theoretical calculation.

3.2 Mechanism of Fe(III)-EDDS photodegradation

Taking into account the first published results on the octahedric structure of the complex Fe(III)-EDDS [18], on the photo-reactivity of iron complexes [19] and the chemical structure of EDDS with the two different environments of carboxylate groups ($^{\cdots}HC—COO^{-}$) and ($^{\cdots}HC—CH_2—COO^{-}$), we propose a mechanism of EDDS oxidation with two different ways.

The primary step, after the absorption of a photon by the Fe(III)-EDDS complex, implies a redox process between Fe(III) and one carboxylate group (ligand to metal charge transfer (LMCT) process), yielding to Fe(II) and two different carboxylate radicals ($^{\cdots}HC—COO^{\bullet}$) and ($^{\cdots}HC—CH_2—COO^{\bullet}$). These two radicals undergo a very fast decarboxylation giving rise to two radicals centered on a carbo atom, one primary radical ($^{\cdots}HC—CH_2^{\bullet} = R^{\bullet}$) and one secondary radical ($^{\cdots}HC^{\bullet} = R'^{\bullet}$) and these radicals react with oxygen to form peroxy radicals $ROO^{\bullet}$. From these peroxy radical, mono and bimolecular reactions are described in detail [28]. The hypothesis, that bimolecular reaction is favored in aqueous solution for primary and

secondary peroxy radicals leading to the formation of intermediate compound called tetroxide, is strongly supported [29]. The decomposition of this instable intermediate to give molecular oxygen and two alkoxy radicals is a well-known reaction [28]. The first part of the mechanism is detailed in the following mechanism (scheme 1).

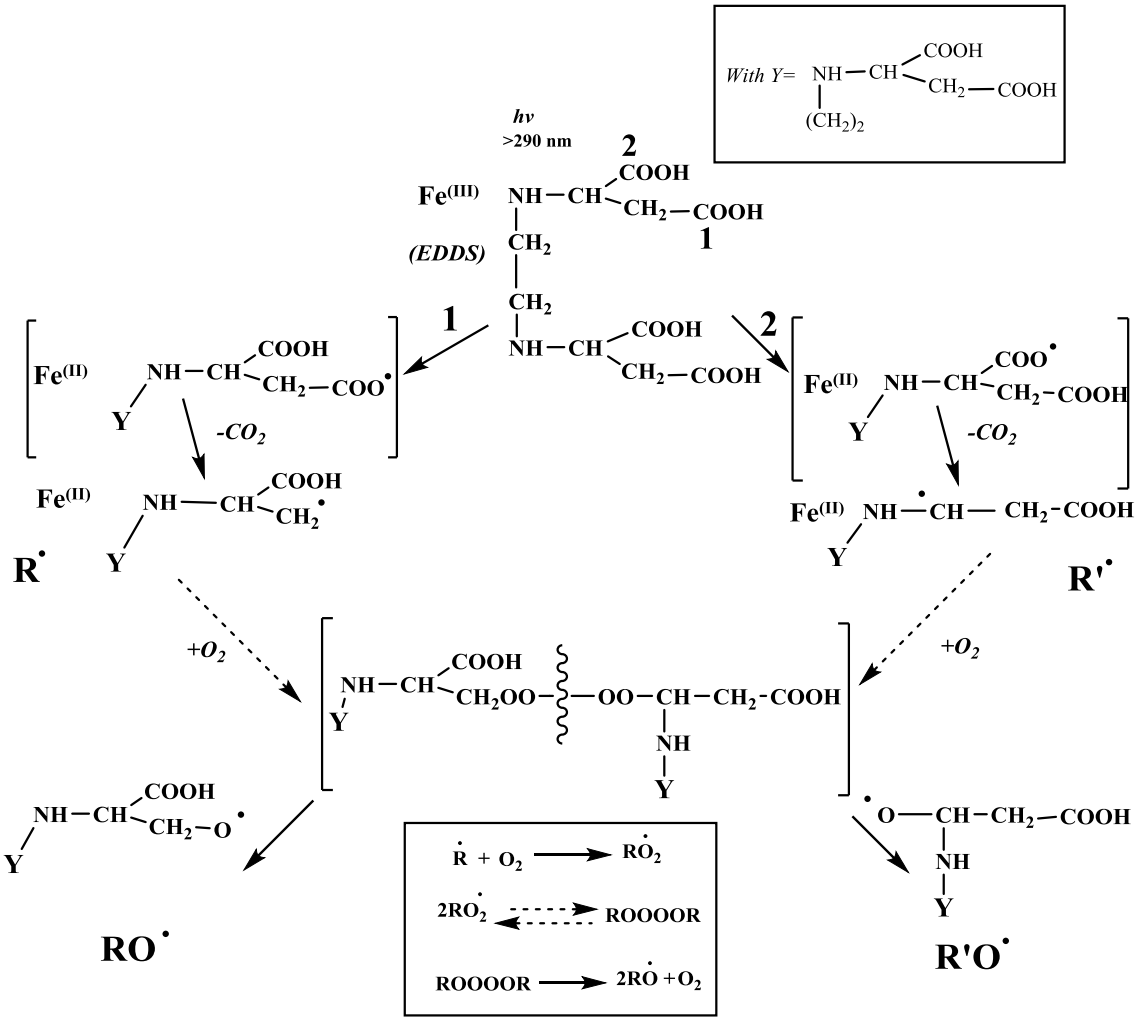

Scheme 1: First part of the mechanism of Fe(III)-EDDS complex photodegradation

The two alkoxy radicals RO$^{\bullet}$ and R'O$^{\bullet}$ from the primary and secondary radical generated in ways 1 and 2 respectively can undergo β-scissions [28].

From the radical RO$^{\bullet}$ (scheme 2, way 1), the β-scission of the C—H bond gives rise to the formation of one compound with an aldehyde function corresponding to the molecular formula of the product (d) identified by MS analysis and a H$^{\bullet}$ radical. The scission of the C—C bond of the radical RO$^{\bullet}$ (scheme 2, way 1) leads to the formation of a new secondary

radical. The recombination of this radical with the H radical corresponds to the formation of product with the molecular formula of the identified product (a) (scheme 2, way 1). This new secondary radical can also react with oxygen to give a new peroxy radical, and with the same reactions sequence than in scheme 1, a new alkoxy radical. Finally, β-scissions of C-C bonds of this alkoxy radical gives rise to the formation of one compound with an aldehyde function and two compounds with acid carboxylic function. One of these two compounds has a molecular formula of the product (c) identified by HRMS analysis (scheme 2, way 1).

From the radical R'O$^{\bullet}$ (scheme 2, way 2), the β-scission of the C—H bond leads to the formation of a product with one amide function corresponding to m/z mass and the molecular formula of the product (d) like in the way 1 from the radical A. However, the chemical formula is not the same; it is a regio-isomer. The two other β-scissions from C—N and C—C bonds of the radical R'O$^{\bullet}$ (scheme 2, way 2) lead to two products with aldehyde function but not identified during our MS analysis.

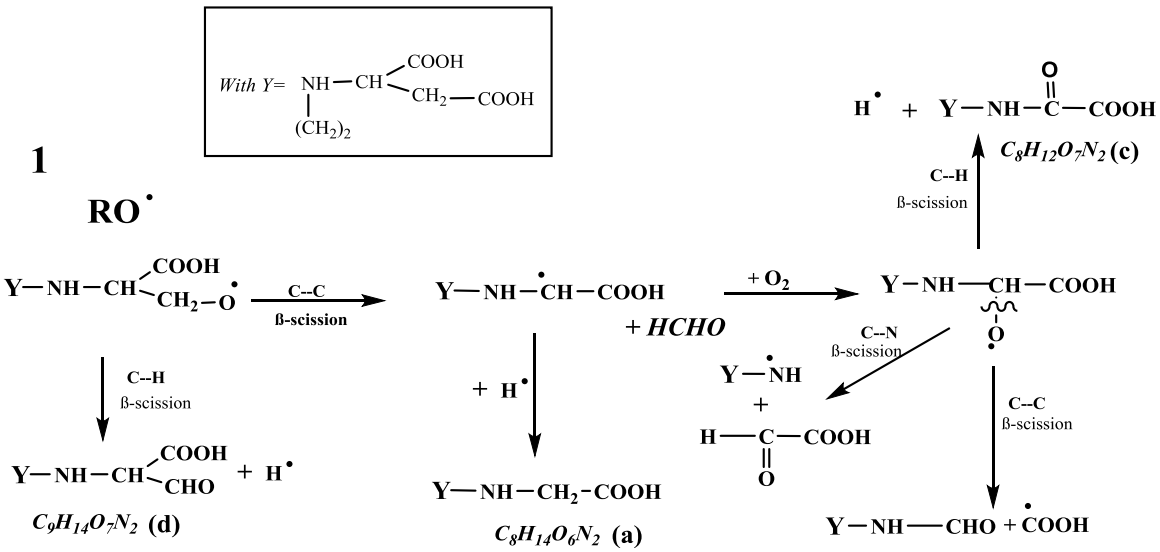

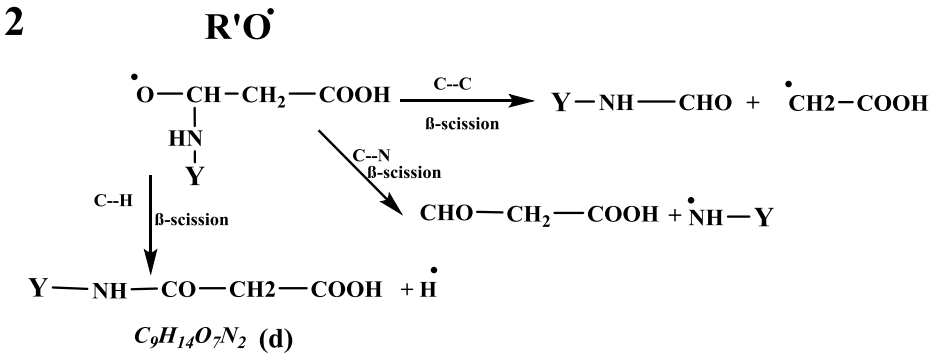

Scheme 2: Mechanism from alkoxy radicals (RO• and R'O•) formed in the ways 1 and 2 (scheme 1)

The other detected by-products, with a lower intensity by HRMS analysis, cannot be explained with the first part of the mechanism. The molecular formulas of products f, g and k can be found from the photochemical degradation of the product Y—NH—CHO formed from both the primary and secondary radicals i.e. ways 1 and 2 (Scheme 2). The same reactivity with the two radicals (primary and secondary) can be proposed on the two carboxylic functions still present in the compound Y—NH—CHO. The detailed of this mechanism is depicted in Scheme 3.

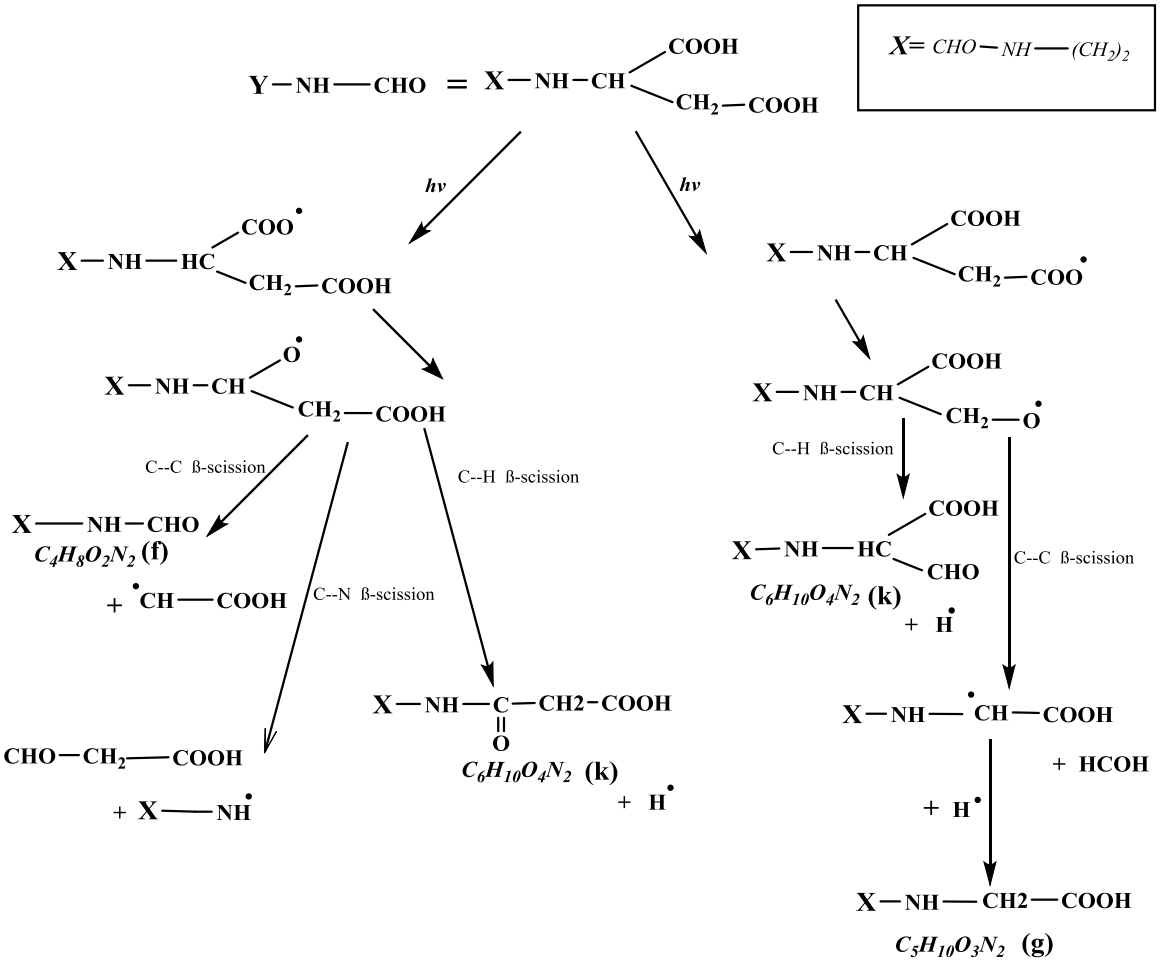

Scheme 3: Mechanism from the product Y—NH—CHO *formed in the first part in the two ways of EDDS transformation (scheme 2). Note that Y—NH—CHO (scheme 2) and X-NH-CH(COOH)-(CH_2COOH) (scheme 3) are the same compound CHO- NH-(CH_2)$_2$- NH-CH(COOH)-(CH_2-COOH)*

3.3 Molecular modeling studies on radical stability

The molecular modeling studies were performed on the stability of primary R$^\bullet$ and secondary R'$^\bullet$ radicals obtained after the LMCT process and the very fast decarboxylation. The molecular structures obtained from the calculations are presented in Figure 4. DFT calculations demonstrate that the secondary radical is the most stable with a difference of -64.2 kJ relative to the primary radical (Table 2). So, the primary radical will be more reactive than the secondary radical, however this result does not give information on the relative rates

of formation of these two radicals. The predominant product will be the one that will be formed with the higher rate during the photo redox process.

4. Conclusion

We present here the first scheme of the mechanism of photochemical degradation of Fe(III)-EDDS complex which remained unknown in spite an intensive use of this iron complex.

All the main by-products formed and identified by HRMS analysis can be explained by the photochemical mechanism involving a LMCT process. These results demonstrate the transfer of electron between the metal and the ligand through the carboxylic acid function. After that the ligand is oxidized leading to the formation of different compounds. Two different oxidation pathways can be distinguished depending on the type of carboxylic acid involved in the redox process. Even if the primary radical is more stable and leads to the formation of the 2 most intense products in HRMS analysis (c) and (d) it is not possible to conclude about the priority in the course of the mechanism. Further modeling studies should be performed to better understand the decarboxylation process of the excited states and determine which radical is formed first. The formation of the more intense by-product (c) detected by HRMS analysis can be only explained from the primary radical ($\mathbf{R}^{\bullet}$). Finally, all the by-products identified have a lower molecular mass than EDDS and correspond to shorter oxidized products with formation of new aldehyde, carbonyl or carboxylic acid functions. We are in the presence of a multi-step process of chain fragmentation with a shortening by oxidation. The proposed mechanism, based on HRMS data show that it is similar to that proposed for Fe(NTA) phototransformation. Among to the shorter oxidized products, formaldehyde is produced (schemes 2 and 3) which is likely to be further oxidized to formic acid. These C1– compounds are more easily biodegradable and so less toxic for aquatic environment. This study suggests that the use of EDDS involved in the different advanced oxidation processes

using iron like Fenton or photo-Fenton used for water treatments would not induce major toxicity risk for the aquatic environment.

Acknowledgements:

This work was funded by the French ANR program BIOCAP (N° ANR-13-BS06-004-01). It was also supported by the French Ministry and CNRS. The authors acknowledge the financial support from the Fédération des Recherches en Environnement through the CPER founded by Région Auvergne Rhône-Alpes, the French ministry, and FEDER from the European community. S. Jaber is recipient of a grant from the Walid Joumblatt Foundation (WJF) for University Studies, Beirut, Lebanon. Computations have been performed on the supercomputer facilities of the Mésocentre Clermont-Auvergne.

References:

[1] R. A. Peters, L. A. Stocken, R. H. S. Thompson, British Anti-Lewisite (BAL), *Nature*, 1945, 156, 616–619.

[2] S. P. Bessman, H. Ried, M. Rubin, Treatment of lead encephalopathy with calcium disodium versenate; report of a case, *Medical Annals of the District of Columbia*, 1952 Jun; 21(6), 312–315.

[3] C. Oviedo, J. Rodriguez, EDTA: the chelating agent under environmental scrutiny, Quimica Nova, 2003, 26(6), 901-905.

[4] M. W. H. Evangelou, M. Ebel, A. Shaeffer, Chelate assisted phytoextraction of heavy metals from soil. Effect, mechanism, toxicity, and fate of chelating agents, *Chemosphere*, 2007, 68, 989-1003.

[5] J. Li, G. Mailhot, F. Wu, N. Deng, Photochemical efficiency of Fe(III)-EDDS complex : OH radical production and 17β-estradiol degradation, *Journal of Photochemistry and Photobiology A:Chemistry*, 2010, 212, 1-7.

[6] W. Huang, M. Brigante, F. Wu, C. Mousty, K. Hanna, G.Mailhot, Assessment of the Fe(III)-EDDS complex in Fenton-like processes from the radical formation to the degradation of bisphenol A, *Environmental Science and Technology*, 2013, 471952-1959.

[7] B. Kos and D. Leštan, Influence of a biodegradable ([S,S]-EDDS) and nondegradable (EDTA) chelate and hydrogel modified soil water sorption capacity on Pb phytoextraction and leaching, *Plant Soil*, 2003, 253, 403–411.

[8] J. S. Jaworska, D. Schowanek and T. C. J. Feijtel, Environmental risk assessment for trisodium [S,S]-ethylene diamine disuccinate, a biodegradable chelator used in detergent applications, *Chemosphere*, 1999, 38, 3597–3625.

[9] M. Bucheli-Witschel, T. Egli, Environmental fate and microbial degradation of

aminopolycarboxylic acids, FEMS Microbiology Reviews, 2001, 25, 69-106.

[10] S. Tandy, A. Ammann, R. Schulin and B. Nowack, Biodegradation and speciation of residual SS-ethylenediaminedisuccinic acid (EDDS) in soil solution left after soil washing, *Environ. Pollut.*, 2006, 142, 191–199.

[11] P. C. Vandevivere, H. Saveyn, W. Verstraete, T. C. J. Feijtel and D. R. Schowanek, Biodegradation of metal-[S,S]-EDDS complexes, *Environ. Sci. Technol*., 2001, 35, 1765–1770.

[12] L. Clarizia, D. Russo, I. Di Somma, R. Marotta, R. Andreozzi, Homogeneous photo-Fenton processes at near neutral pH : A review, *Applied Catalysis B: Environmental*, 2017, 209, 358-371.

[13] Y. Zhang, M. Zhou, A critical review of the application of chelating agents to enable Fenton and Fenton-like reactions at high pH values, *Journal of Hazardous Materials*, 2019, 362, 436-450.

[14] Y. Wu, M. Passananti, M. Brigante, W. dong, G. Mailhot, Fe(III)-EDDS complex in Fenton and photo-Fenton processes : from the radical formation to the degradation of a target compound, *Environmental Science and Pollution Research*, 204, 21, 12154-12162.

[15] N. Klamerth, S. Malato, A. Aguear, A. Fenandez-Alba, G. Mailhot, Treatment of municipal wastewater treatment plant effluents with modified photo-Fenton as a tertiary treatment for the degradation of micro pollutants and disinfection, Environmental Science and Technology, 2012, 46, 2885-2892.

[16] A. Bianco, M.I. polo-Lopez, P. Fernandez-Ibanez, M. Brigante, G. Mailhot, Disinfection of water inoculated with *Enterococcus faecalis* using solar/fe(III)EDDS-H_2O_2 or $S_2O_8^{2-}$ process, Water Research, 2017, 118, 249-260.

[17] Y. Wu, A. Bianco, M. Brigante, W. Dong, P. de Sainte Claire, K. Hanna, G. Mailhot,

Sulfate radical photogeneration using Fe-EDDS : influence of critical parameters and naturally occurring scavengers, *Environmental Science and technology*, 2015, 49, 14343-14349.

[18] Y. Wu, M. Brigante, W. Dong, G. Mailhot, toward a better understanding of Fe(III)-EDDS photochemistry: theoretical stability calculation and experimental investigation of 4-*tert*-butylphenol degradation, The journal of Physical chemistry A, 2014, 118, 396-403.

[19] O. Abida, G. Mailhot, M. Litter, M. Bolte, Impact of iron-complex (Fe(II)-NTA) on photoinduced degradation of 4-chlorophenol in aqueous solution, Photochemical and Photobiological Sciences, 2006, 5, 395-402.

[20] W. Huang, Homogeneous and heterogeneous Fenton and photo-Fenton processes: Impact of iron complexing agent Ethylenediamine-N,N'-disuccinic acid (EDDS), PhD Thesis, no DU 2241, Université Blaise Pascal, Clermont-Ferrand (France).

[21] http://gaussian.com/citation_b01/

[22] P. Hohenberg, W. Kohn, Inhomogeneous electron gas, Physical Review, 1964, 136, B864–B871.

[23] W. Kohn, L.J. Sham, Self-consistent equations including exchange and correlation effects, Physical Review, 1965, 140, A1133–A1138.

[24] A.D. Becke, Density-functionnal thermochemistry. III. The role of exact exchange, The Journal of Chemical Physics, 1993, 98, 5648–5652.

[25] C. Lee, W. Yang, R.G. Parr, Development of the Colle-Salvettu correlation-energy formula into a functional of the electron density, Physical Review, 1988, 37, B785–B789.

[26] S.H. Vosko, L. Wilk, M. Nusair, Accurate spin-dependent electron liquid correlation energies for local spin density calculations: a critical analysis, Canadian Journal of

Physics, 1980, 58, 1200–1211.

[27] J. Tomasi, B. Mennucci, and R. Cammi, “Quantum mechanical continuum solvation models,” Chemical Review, 2005, 105, 2999-3093.

[28] C. Von Sonntag, H-P. Schuchmann, The elucidation of peroxyl radical reactions in aqueous solution with the help of radiation-chemical methods, Angewandte Chemie International Edition, 1991, 30, 1229-1253.

[29] J.E. Bennett, J.A. Howard, Bimolecular self-reaction of proxy radicals. An oxygen-18 isotope study, 1973, 95(12), 4008-4010.

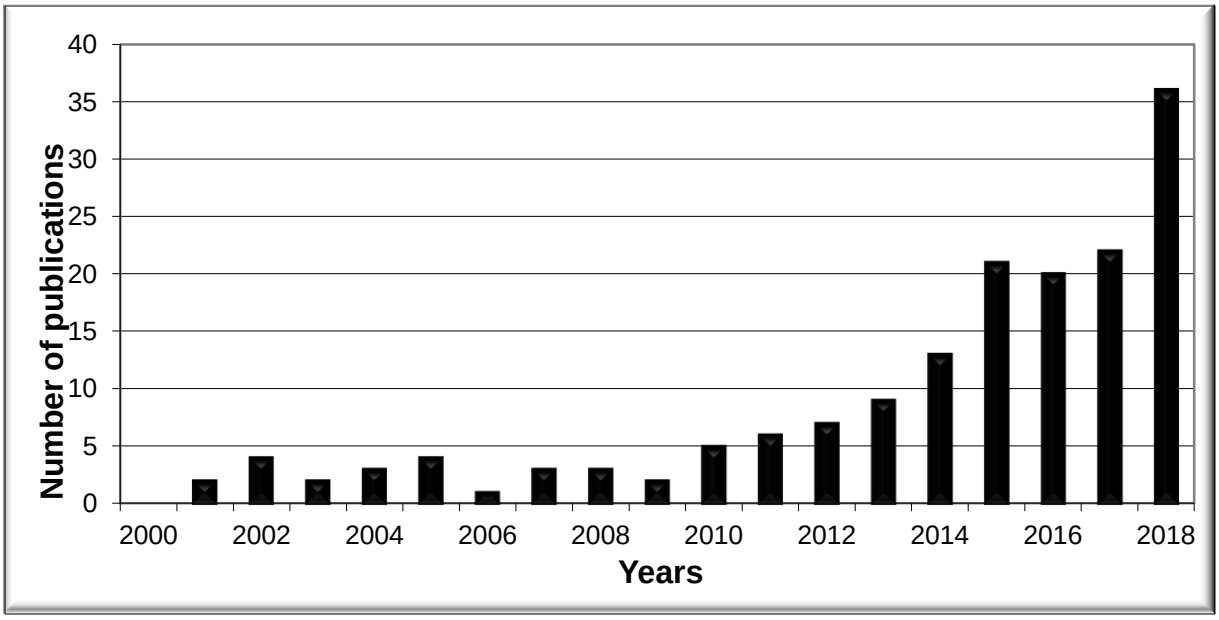

Figure 1: Productivity of scientific papers with the words “Fenton” and “EDDS” in the main topic (data source: ScienceDirect)

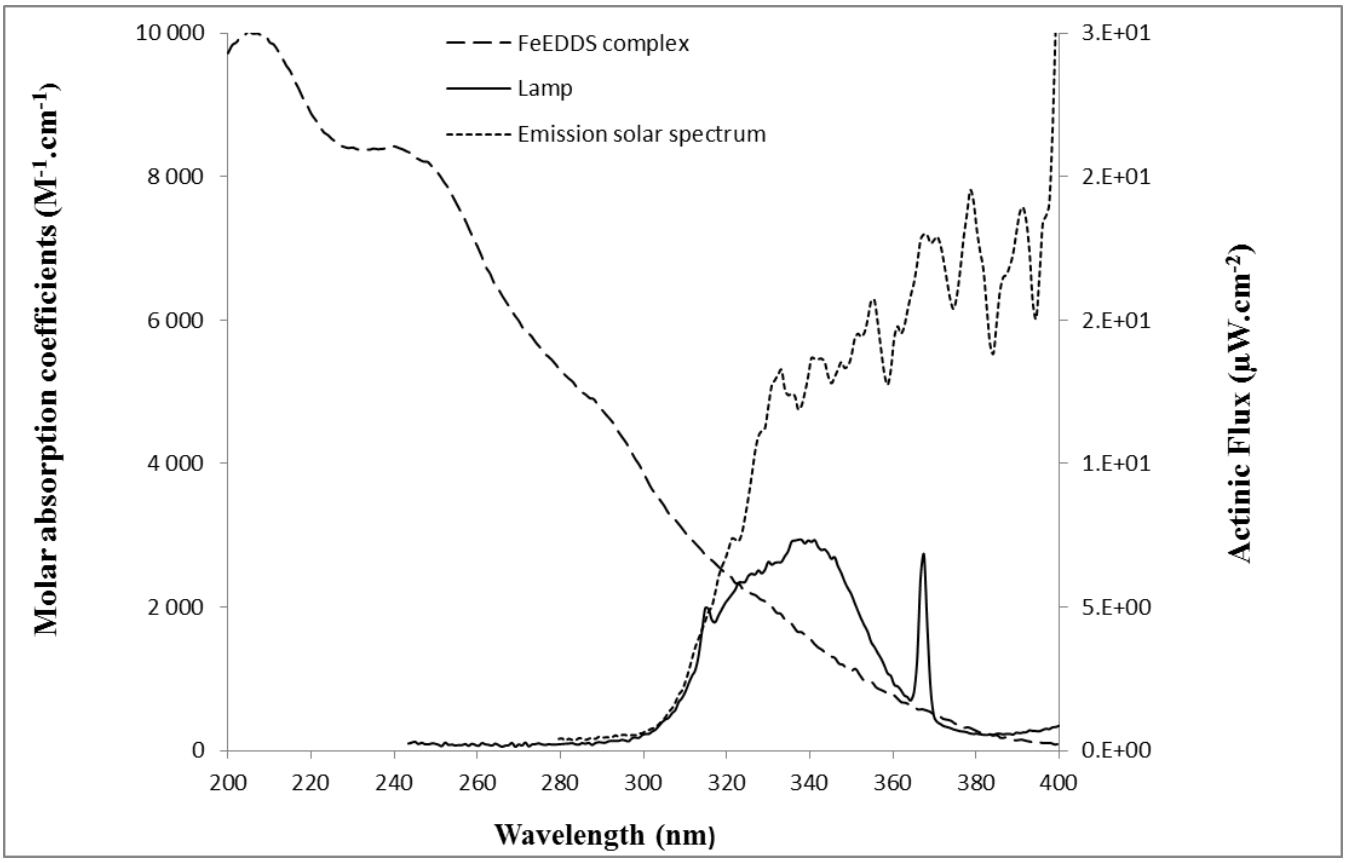

Figure 2: Comparison of the actinic flux of the lamps used and the emission of the solar spectrum below 400 nm. Molar absorption coefficients of the aqueous solution of Fe(III)-EDDS complex.

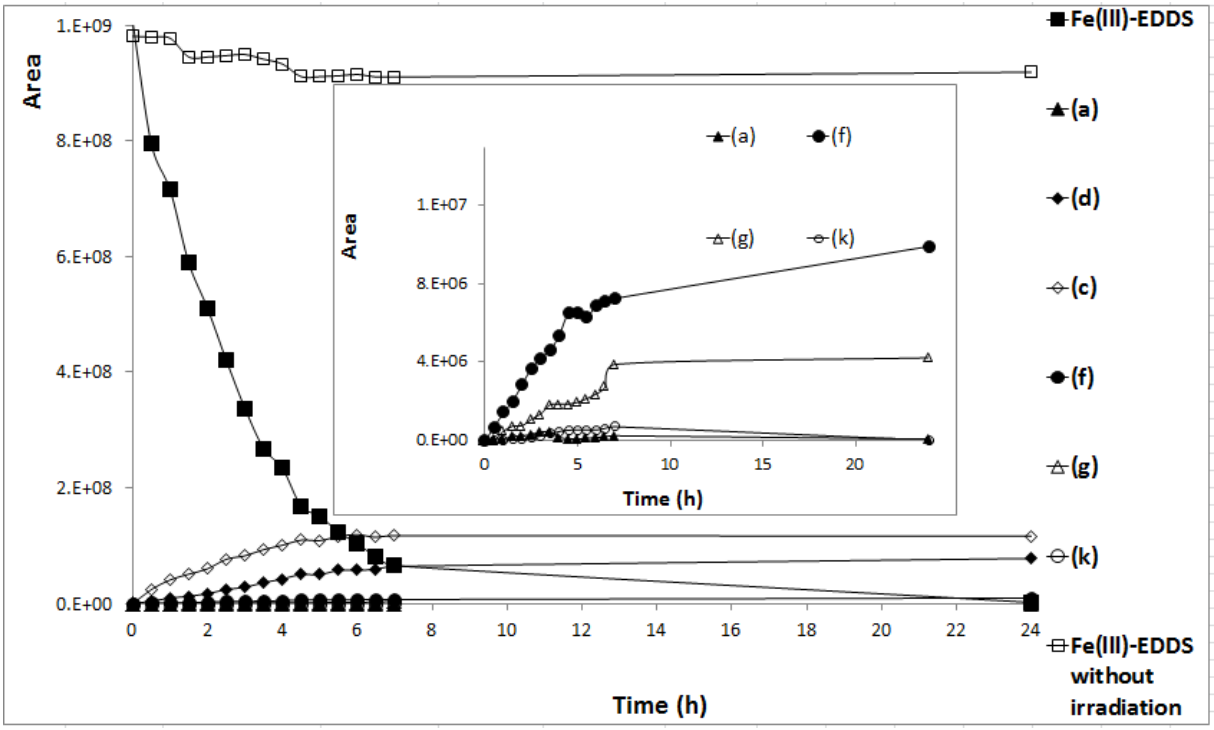

Figure 3: Kinetics of the photodegradation of the complex Fe(III)-EDDS and of the formation of the detected byproducts. Insert: zoom on the formation of the lowest detected byproducts. Initial [Fe(III)-EDDS] = 0.5 mM

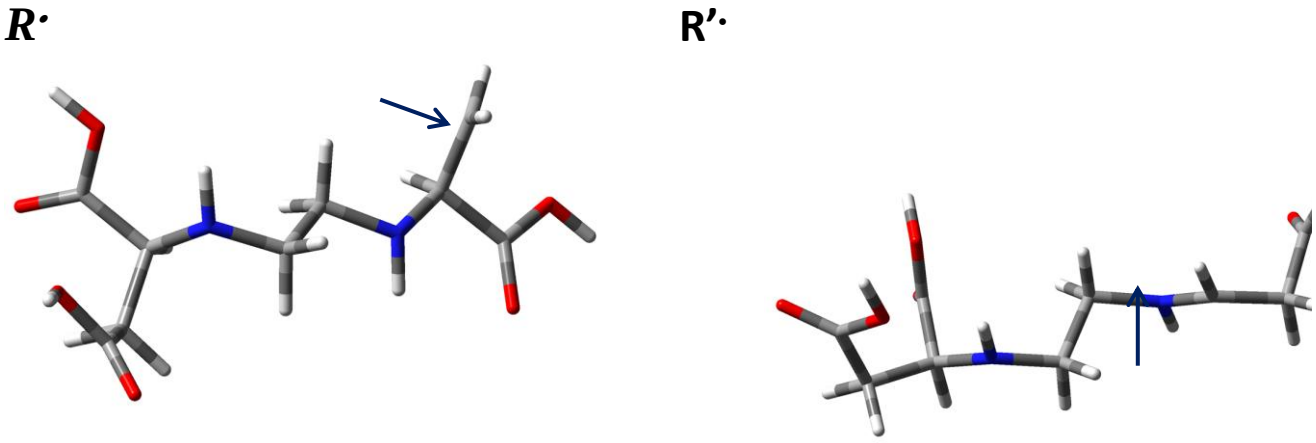

Figure 4: Representation of the molecular structure of the two alkyl radicals (primary **R$^{\bullet}$** and secondary **R'$^{\bullet}$** in scheme 1) used for the calculations. The localization of the radical is indicated by an arrow.

Table 1: Characterization of the Fe(III)-EDDS complex, EDDS and the six main photo-products from UPLC-HRMS analyses

Name	*Molecular Formula*	*Exact mass*	*Retention time(min)*	*ionization Mode*	*Adduct*	*Isotopic Ratio*
FeEDDS[1]	$FeC_{10}H_{13}O_8N_2$	345.00209	0.64	M+H		344.0131(5.9) ; 346.0082(100)
				346.0086		347.0109(13.54) ; 348.0124(2.83)[2]
EDDS	$C_{10}H_{16}O_8N_2$	292.09067	0.6	M+H		
				293.0959		
(d)	$C_9H_{14}O_7N_2$	262.0801	0.63	M-H	M+Cl	261.0726(100) ; 262.0759(9.75)[2]
				261.0726	298.0567	
(c)	$C_8H_{12}O_7N_2$	248.06445	0.65	M+H	$M+NH_4$	249.0710(100) ; 250.07461(8.72)[2]
				249.071	265.091	
(a)	$C_8H_{14}O_6N_2$	234.08519	0.61	M-H	M+Cl	233.0307(100) ; 234.0346(5.81)[2]
				233.0307	270.0429	
(k)	$C_6H_{10}O_4N_2$	174.06406	0.59	M+H	M+Na	Not detected
				175.0707	196.1076	
(g)	$C_5H_{10}O_3N_2$	146.06914	0.61	M+H	$M+NH_4$;M+K	147.0760(100) ; 148.0605(7.70)[2]
				147.076	163.1224 ; 184.152	
(f)	$C_4H_8O_2N_2$	116.05858	0.8	M+H	$M+NH_4$;M+Na	117.0659(100) ; 118.0502(2.7)[2]
				117.0659	133.0759 ; 138.0574	

[1] Fe(III)-EDDS is the standard used in UPLC-HRMS measurements. [2] The isotopic distribution of iron and carbon, for Fe(III)-EDDS complex and their photo-products are presented in the form of spectra in the supplementary material section (Figures S8-S13).

Table 2: Energies and energy gaps of the two radicals

	Primary alkyl radical (**R$^{\bullet}$**)	Secondary alkyl radical (**R'$^{\bullet}$**)
$E_{B3LYP/6\text{-}31g}$ (Hartree)	-912.503969653	-912.529111078
$E_{\text{Free Gibbs}}$ (Hartree)	-912.303341	-912.327837
$\Delta E_{\text{Free Gibbs}}$ (kJ)	0,0	-64,25